ACS OMEGA

Open Access

http://pubs.acs.org/journal/acsodf

Article

Molecular Simulation of Surfactant Displacement of Residual Oil in Nanopores: Formation of Water Channels and Electrostatic Interaction

Lipei Fu, Yuan Cheng, Kaili liao,* Zhanqi Fang, Minglu Shao, Jiyun Zhu, Ziqiang Xu, and Yanyu Xu

Cite This: *ACS Omega* 2024, 9, 4085−4095

Read Online

ACCESS | Metrics & More | Article Recommendations

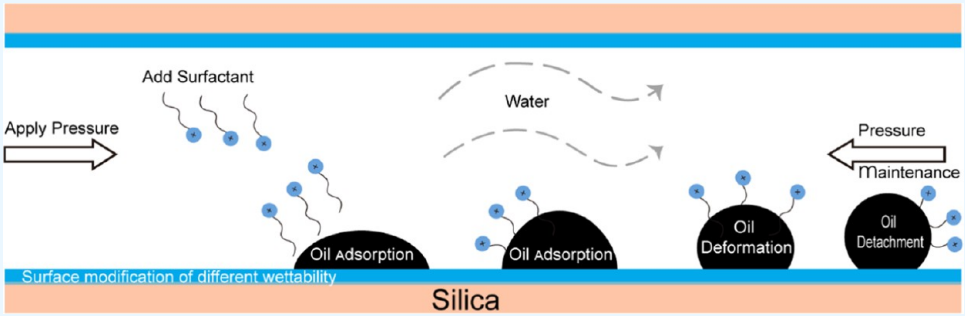

ABSTRACT: The water−oil−rock system's surfactant and electrostatic interactions are essential for removing oil droplets from rock substrates. Our work illustrates the impact of surface charge on the oil contact angle in an ideal system comprising silica, water, and dodecane; smaller contact angles are observed for more polar substrates. Modifying the polarity of the model silica surface allows for the observation of the creation of heteromolecule channels and the process of stripping crude oil while accounting for the impacts of water flow and different types of surfactant molecules. In solutions containing ionic surfactants, the injection and diffusion of water molecules between the oil layer and the silica substrate are facilitated by the disturbance of the oil molecules by the surfactant molecules. By comparing different surfactants in water flow, the characterization of water molecular channels and the stripping process of crude oil can be observed. The disruption of oil molecules by the surfactant molecules has been found to enhance the injection and diffusion of water molecules between the oil layer and the silica substrate in solutions containing ionic surfactants. The size of the contact angle and the extension of the water channel are simultaneously greatly influenced by the surfactant's molecular characteristics and the substrate's polarity. These simulation results show that several factors influence the process of water molecule channel creation that water molecules diffuse, and the detachment of oil from the silica substrate is facilitated by the migration of surfactants to the bottom of the oil molecule and the electrostatic interactions between the water molecules and the silica substrate.

1. INTRODUCTION

It is crucial to understand the processes by which crude oil separates on rock surfaces in the oil production sector.[1,2] Rock formation in reservoirs is a very complicated process.[3,4] The structure of a reservoir is complex in an actual reservoir environment. Within the porous structure of the internal pore channel, the rock surface is irregular, and oil repulsion is greatly impacted by the surface roughness. Low porosity, low permeability, and low pressure are obstacles that arise when developing tight reservoirs and can have a significant impact on the fluid transport behavior. This could lead to a rapid decline in production and create challenges in replenishing energy supplies during the development process.[5−7] The fluid in nanoscale pores faces increased resistance during the oil displacement process because it must not only overcome viscous resistance but also deal with the fluid's interaction with the pore wall. Figure 1 illustrates the substantial amount of residual oil that is still present in the oil reservoir following the water displacement process. Significant obstacles to oil recovery are the distribution of residual oil and the complex pore-scale structure. The benefits of increasing oil production from pure water drive implementation are not very great.[8] As a result, the displacement fluid usually contains a specific quantity of surfactants or nanoparticles added to it. As Figure

Received: November 15, 2023
Revised: December 27, 2023
Accepted: December 28, 2023
Published: January 10, 2024

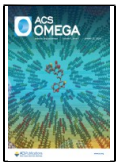

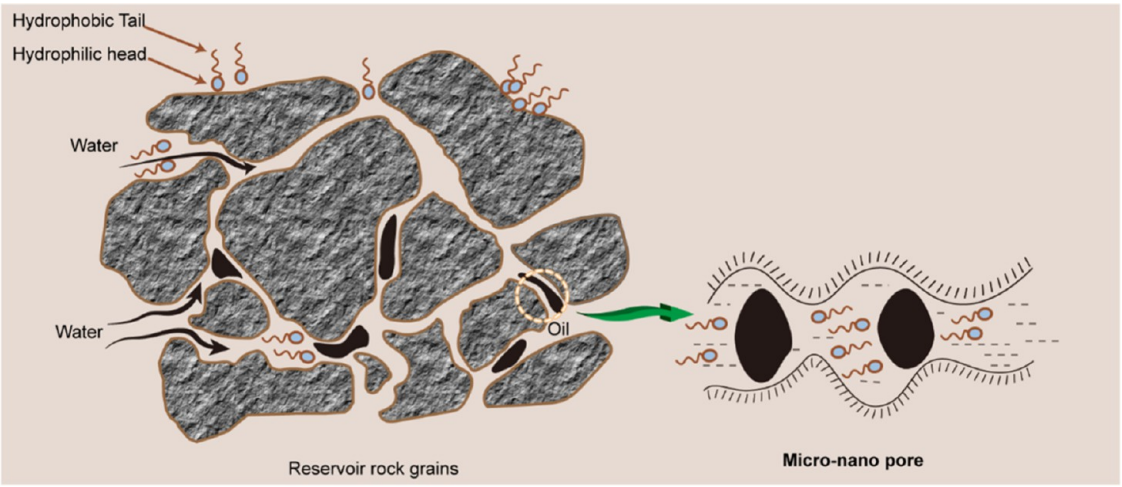

Figure 1. Crude oil distribution and surfactant flooding.

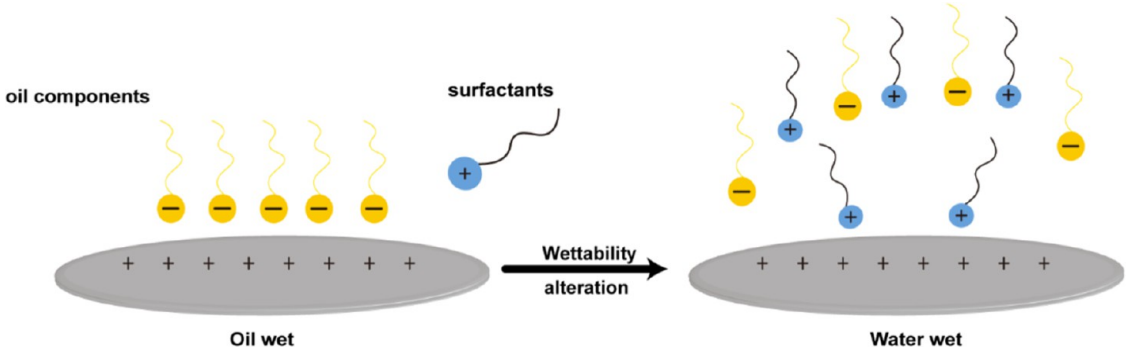

Figure 2. Wettability alteration.

2 illustrates, one of the main functions of surfactants is to lower the interfacial tension between water and oil, which, in turn, lowers the capillary pressure of oil in pore space. The alternative is to alter the surface's wetness, which lessens the adherence of oil droplets to the rock.[9−11]

Using molecular dynamics simulations, numerous researchers have examined gas−liquid and liquid−liquid systems in the context of surfactant oil displacement. Research has indicated that the primary factor propelling various surfactant types during the oil flooding procedure is the decrease in the interfacial tension between the oil and water. The migration patterns and organization of sodium dodecyl sulfate (SDS) at the interfaces between gas/liquid and liquid/liquid were examined by Schweighofer et al.[12] According to their research, SDS molecules have different orientations in these two systems, which significantly affect how amphiphiles are oriented in denser monolayers. Using molecular dynamics simulations, Li et al. looked into how pH and surfactant type affected the water/octadecane interfacial tension.[13] They discovered that the interfacial tension between water and octadecane was reduced when the pH was raised. Ahmadi et al.,[14] using a dissipative dynamics simulation, determined how the water/oil surfactant system's interface was affected by temperature, salt content, water/oil ratio, shear rate, and surfactant type. Shi et al.'s study[15] employed four surfactants to investigate their microscopic behavior at the oil−water interface. It was found that while Gemini had the greatest effect, all four surfactants were able to form stable monomolecular layers there. There are not many results from modeling nanopores for fluid−solid interfaces.

Enhancing oil recovery during secondary water injection by altering wettability with surfactant addition,[16] and surfactant molecules can disrupt the layer of adsorbed oil molecules that have developed on the solid surface in fluid−solid systems. This may cause the oil molecules to become more perturbed and more easily detached from the solid wall.[17,18] Kochijashky et al.[19] studied how a three-phase contact line's spontaneous contraction can separate oil droplets from a glass substrate. Zhang et al. observed that when micellar nanofluids were used to replace hexadecane in glass capillaries, the droplets eventually separated from the capillary surface and formed spherical droplets inside the capillary.[20] Li et al.[21] examined the impact of temperature, surfactant concentration, and calcium ion concentration on the separation of oil from carboxyl-modified silica surfaces in cetyltrimethylammonium bromide (CATB) surfactant solutions. Many scholars have also studied the effectiveness of chemical flooding in oil recovery. For example, Druetta et al.[22] investigated the effect of physical properties of surfactants in oil recovery, Tavakkoli et al.[23] enhanced the oil-repellent performance of surfactants by adding nanoparticles, Liu et al.[24] investigated the effect of different surfactant concentrations in oil repulsion, and Nafisifar et al.[25] demonstrated that surfactants can change interfacial tension. However, research on the surface charge of rock is limited.

Molecular dynamics (MD) simulation is an effective method for studying oil drive mechanisms at the microscopic level.

https://doi.org/10.1021/acsomega.3c09116
ACS Omega 2024, 9, 4085−4095

Using MD calculations based on experimental data, Jang et al.[26] examined the interfacial characteristics and adsorption behavior of several isomeric sodium dodecyl benzenesulfonate (SDBS) molecules at the decane/water interface. For the study of residual oil in the nanopore, Tang et al.[27] demonstrated the deformation of the oil molecules under the action of surfactants until the surface oil molecules were detached from the rock surface by using various surfactants to separate the residual oil in the pore space. Tang et al.[28] investigated the separation process of oil molecules on a horizontal substrate, detailing the process of water channel formation and swelling. The formation of water channels was found to be significantly impacted by surfactants, electrostatic interactions, and the water flow rate.

Due to the mutual repulsion caused by Coulomb forces, the addition of an anionic surfactant can effectively reduce the residue of surfactant in the reservoir because the majority of the clay particles in the reservoir are negatively charged. Surfactants are soluble in polar molecules such as water and have both hydrophilic and lipophilic qualities that allow them to cling to oil molecules while also successfully lowering the interfacial tension between water and oil. Takamura experimented to confirm the activity of ionic surfactants at the interface and to confirm the decrease in interfacial tension following the addition of surfactants to the reservoir.[29] The mechanism by which surfactants work to lower thick oil viscosity at the macromolecular level has not been thoroughly studied. Consequently, to thoroughly and theoretically investigate the mechanism of surfactant oil repellent, as well as to offer theoretical support and direction for oil-repellent production and experiments, this paper chooses the common anionic surfactants (SDBS) and cationic surfactants (DTAB) in production and studies them using molecular dynamics simulation.

In the study of tertiary oil recovery using molecular simulation techniques, many studies have focused on the oil/water interface and there are few studies on the effect of solid/liquid interface properties. Especially in the influence of surfactants on interfacial properties, the interfacial behavior of the oil/water interface has been fully studied and relatively perfect theory, while solid/liquid interface research is lacking. This paper establishes three types of nanopore models (COM, CVFF, and INT, respectively) based on the current state of research under real temperature and pressure conditions. Table 1 displays detailed surface atomic charge information. The three stages of oil recovery are studied using nonequilibrium kinetic means, and the impact of surfactants on the replacement of various reservoir conditions is examined. This is instructive for understanding the mechanism of the crude oil stripping mechanism from solid surfaces and the replication mechanism in nanopore channels.

Table 1. Charge Values of SiO_2 Surface Atoms from Different Force Fields

force field	surface atoms	charge
COMPASS	Si	0.890
	O	−0.472
	H	0.250
CVFF	Si	0.738
	O	−0.569
	H	0.350
INTERFACE	Si	1.100
	O	−0.675
	H	0.400

2. SIMULATION METHODS AND DETAILS

2.1. Model Construction. As shown in Figure 3, the simulation models were initially configured with two-phase fluids confined between two parallel solid plates with rigid plates (Cu) placed on the left and right. Each simulation system is divided into two parts: a fixed (solid) part composed of nanoslit pore walls and a moving (fluid) part composed of surfactant/oil/water separation mixtures. Each of the two walls within each nanochannel was made up of flat slabs of α-quartz (α-SiO_2), each measuring 298 Å in length. The simulation box's geometry measured 24.6 Å in the y-axis direction. The composition of the liquid phase is as follows: 10,000 molecules of water, 100 molecules of n-dodecane ($C_{12}H_{26}$) oil, and 20 molecules of surfactant (DTAB or SDBS), distributed randomly in the water on the left side of the oil molecule. In addition, by saturating the dangling O atoms with H atoms, the exposed (001) surface functions as a contact surface and creates a hydroxylated surface.[30] To study the effect of surface polarity on oil displacement, we have chosen three atomic charge sets, which are center-of-mass (COM), CVFF, and INT, respectively, as shown in Figure 3d. Three atomic charge sets for Si, O, and H atoms on a silicon substrate were derived from the COMPASS (condensed-phase optimized molecular potentials for atomistic simulation studies),[31] CVFF (consistent valence force field),[32] and INTERFACE force field,[33] respectively. The specific setting of the charge is shown in Table 1.

2.2. Software and Force Field. A fixed (solid) part was generated by using the Material Studio 2022 (MS) package. The liquid phase was established by the PACKMOL (version 20.3.5) software[34] and the Moltemplate (version 2.20.14) software. The Packmol was used for modeling Protein Data Bank (PDB) files; hereafter, the Moltemplate software constructed data files, which were used as the input file of LAMMPS. Details of the steps of the simulation are shown in Figure 4.

In this study, all of the organic molecules were parametrized using the Polymer Consistent Force Field (PCFF), and, the SPC/E[35] model was used for water molecules. The $-C-SO_3$, $-N-(CH_3)_3$ can also be well described by PCFF, a widely used all-atom force field that has been validated to be capable of accurately predicting structural and thermodynamic properties for a broad range of organic and inorganic compounds. The PCFF, whose parameters were determined through ab initio calculation, is appropriate for both organic and inorganic molecules that possess both binding and nonbinding potential functions. The PCFF or INTERFACE force field served as the basis for the force field parameters of nanoslit hole wall SiO_2, which proved to be highly appropriate for the dynamic simulation of amorphous SiO_2 and the water system. Equation 1 provides the total energy, taking into account both the intermolecular and nonintermolecular interactions

$$E_{total} = E_{bond} + E_{angle} + E_{dihedral} + E_{torsion} + E_{vdW} + E_{Coulombic} \quad (1)$$

where E_{total}, E_{bond}, E_{angle}, $E_{dihedral}$, $E_{torsion}$, E_{vdW}, and $E_{Coulombic}$ are the total energy, bond-stretching, angle-bending, dihedral

https://doi.org/10.1021/acsomega.3c09116
ACS Omega 2024, 9, 4085−4095

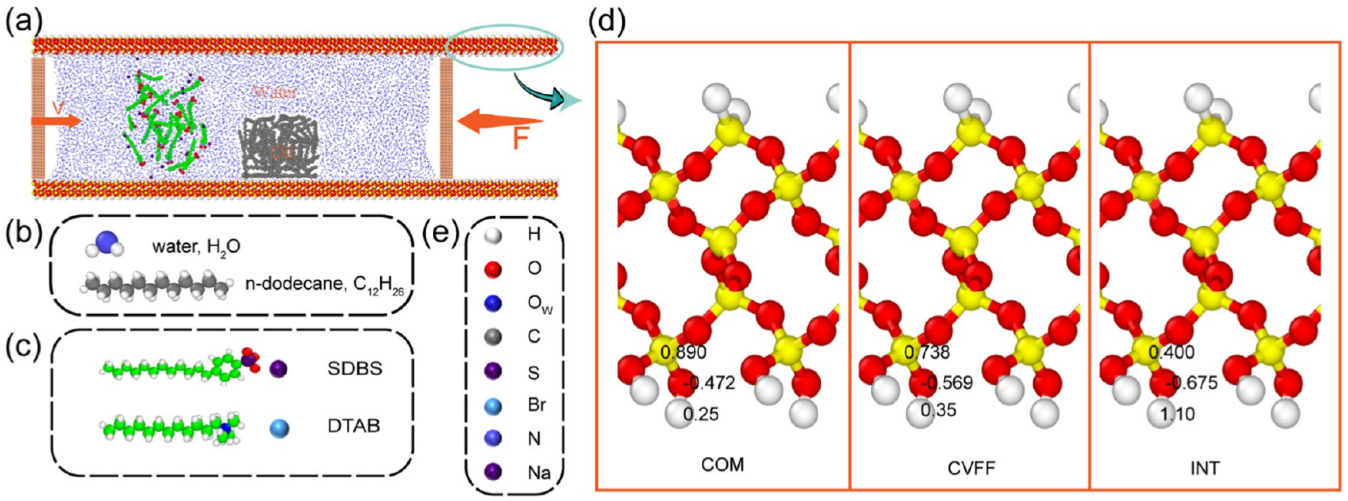

Figure 3. (a) Schematic illustration of the nanoslit model. (b) Water and *n*-dodecane; (c) surfactant; (d) COM, CVFF, and INT, which are three modified surfaces; (e) white, red, blue, gray, purple, cyan, aqua, and modena spheres represent hydrogen, oxygen, oxygen, carbon, sulfur, bromine, nitrogen, and sodium, respectively.

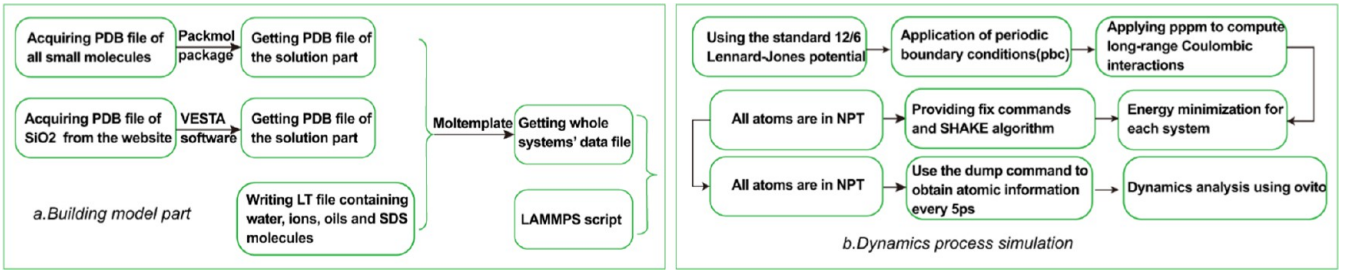

Figure 4. Schematic flowchart of the molecular dynamics simulation.

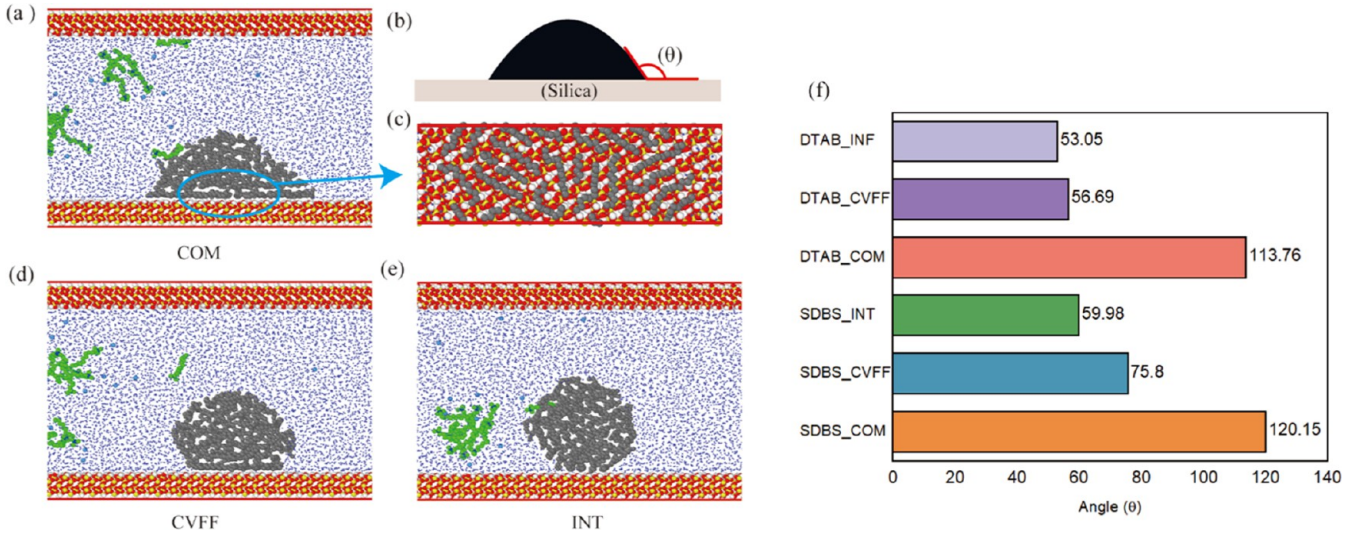

Figure 5. (a, d, e) Adsorption configuration diagrams of crude oil on the three kinds of wall surfaces, respectively. (b) Measurement of the contact angle diagram. (c) Top view of the C12 first layer displayed in CPK mode on the silica surface. (f) Measured contact angle.

energy, torsion energy, van der Waals, and electrostatic components, respectively.

2.3. Molecular Dynamics Simulation (MD). All MD simulations in this paper are performed using the Large-scale Atomic/Molecular Massively Parallel Simulator (LAMMPS) software package.[36] The simulation box dimensions measured 298 × 25 × 94 $Å^3$. In MD simulation, the long-range Coulombic interactions were handled by the particle particle mesh (PPPM) algorithm with a convergence parameter of 10^{-4}, while the short-range van der Waals (vdW) interactions were computed with a cutoff of 12.0 Å. To collect data, the time step and interval were set to 1 fs and 5 ps, respectively. At the beginning of each simulation, an energy minimization was performed to reduce the excessive forces of the system. All subsequent simulations performed a 1 ns equilibrium period under the NVT ensemble with a velocity-rescaling Berendsen

https://doi.org/10.1021/acsomega.3c09116
ACS Omega 2024, 9, 4085−4095

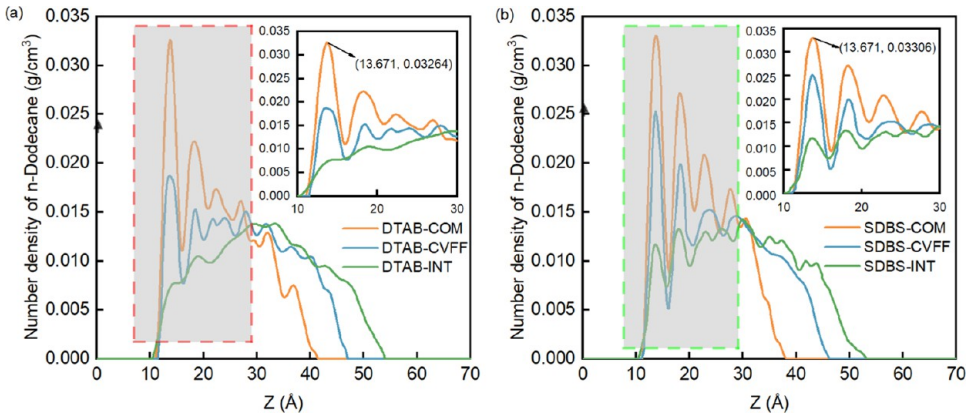

Figure 6. Corresponding number density profiles of *n*-dodecane along the axis normal to the SiO_2 walls (*z*-direction) for all systems: (a) DTAB and (b) SDBS.

thermostat. Periodic boundary conditions are used for all simulations, with an external force applied to the "pressure holding board" to achieve the necessary pressure, at 30 MPa and 330 K. A constant force is applied to the fixed plate on the left during the nonequilibrium molecular dynamics (NEMD) simulation stage. Within the push plate and wall, the relative positions of silicon and oxygen atoms are limited.

3. RESULTS AND DISCUSSION

3.1. Static Contact Angles and Surfactant Characteristics. Understanding the contact angle can help with more precise analysis and prediction of the fluid behavior in the reservoir. The contact angle is commonly used to measure the degree of contact between the oil phase and the formation. Figure 5f shows the contact angle measurements taken during the EMD phase. The angle between the plane of the rock and the tangential direction of the three points of contact among the oil droplets, the rock, and the external environment is known as the static contact angle (Figure 5b). Figure 5 displays the adsorption configurations on the various surfaces (a, d, e). The interface between water and dodecane is visible in this simulation, and every dodecane molecule is grouped into a droplet shape and adsorbed straight onto the rock surface. It should be noted that the droplet's shape is continuously changing at the molecular simulation scale, making it challenging to determine the static contact angle. It was determined to measure the static contact angle every 200 ps for the duration of the EMD simulation (1−2 ns), averaging the results to prevent errors. The contact angle measurements were performed using Digimizer software, version 6.1.1, which was developed by MedCalc Software Ltd. of Belgium. Digimizer is a user-friendly program for analyzing images, enabling the measurement of contact angles, along with other length-related measurements.

It is clear from Figure 5a that there is more interaction between the COM polar surface and the oil droplets and that the oil droplets have a larger contact area on the COM surface. The contact angle varies significantly for different polar surfaces, as indicated by the size of the measurement (Figure 5f). Compared with the oil droplets on the COM surface, the contact angle of the droplets on the INT and CVFF surfaces is substantially smaller. Figure 5a,d,e shows that at 2 s, the silica surface interacts more strongly with the oil molecules on the less polar COM surface, resulting in crescent-shaped adsorption on the rock surface. The larger the charge set of Si and O atoms on the surface of the substrate, the stronger the Coulombic interaction between the water molecules and the silica, and therefore the interaction between the crude oil and the substrate is relatively weaker, resulting in more water molecules entering the oil−water interface, and eventually, the dodecane molecules tend to aggregate into columnar structures. The formation of two more distinct peaks by n-dodecane molecules on the silica surface at Z = 13.67 and 18 Å is depicted in Figure 6, suggesting that the alkane adsorbs on the silica surface form two-layered structures. There is discernible variation in the magnitude of the values on each of the three substrate surfaces, but the number densities nearly invariably form peaks at the same distance. The number density size relationship $N_{com} > N_{cvff} > N_{int}$ is evident from Figure 6. A higher barrier to exfoliation is created by the ordered structure that results from the first peak on the COM surface having a high number density and the alkyl chains remaining flat on the surface (Figure 5c). On the other hand, the first layer of INT is more suited for exfoliation due to its low number density, flat profile, and disorganized alkyl molecule arrangement.

At the start of the EMD phase, surfactant molecules are randomly dispersed within the aqueous phase (Figure 7, left). The micelles' hydrophobic effect causes them to aggregate in less than a nanosecond, owing to their surfactant characteristics (Figure 7, right). Although the degree of aggregation varies, both of these surfactants show some degree of aggregation. DTAB forms small aggregates and exhibits weak intermolecular nonbonding interactions. In aqueous solutions, these small aggregates move more readily, and some of the small molecules migrate to the rock's surface where they adsorb. The primary cause of DTAB's easy electrostatic action adsorption to the negatively charged rock surface is its positively charged headgroup. Conversely, SDBS creates big micelles with an oleophilic core and a hydrophilic outer layer when the hydrophilic groups face the water, and the hydrophobic alkyl chains stay on the inside. The compatibility of oil and water is greatly improved by this amphiphilicity. Reducing surface tension, altering the rock's wettability to allow oil droplets to be readily deformed, lowering the crude oil's flow resistance within rock fissures, and finally allowing water to be swept down are the main goals.

3.2. Surfactant Flooding Dynamic Process. Around 8 ns, at the COM surface, the SDBS micelles break down, dispersing and migrating surfactant molecules on the oil

https://doi.org/10.1021/acsomega.3c09116
ACS Omega 2024, 9, 4085−4095

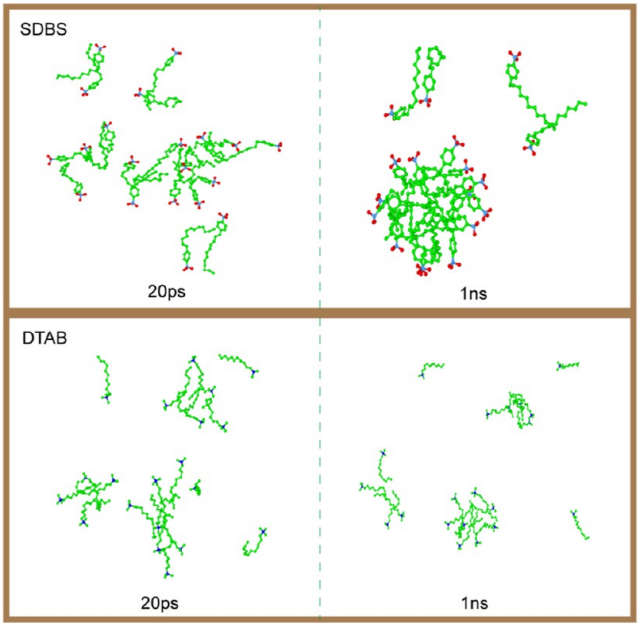

Figure 7. Distribution of the two surfactants in the solution at 20 ps and 1 ns.

aggregate until they cover the entire surface of the oil droplet, creating a stable adsorption layer. The oil droplets slide along the pore wall when a water flow is present. There are comparatively few molecules of the DATB surfactant adsorbed on the crude oil's surface. It is discovered that for the COM port, the oil droplet's shape is resistant to deformation even when its exterior is coated in surfactant. At 5 ns, DTAB first comes into molecular contact with the oil phase on the CVFF surface, and it spreads quickly over the oil droplet's surface. Then, DTAB changes to the oil−water−rock interface after about 9 ns. Meanwhile, as Figure 9b illustrates. after 9 ns, the slope of the curve increases, indicating that DTAB can improve the crude oil displacement efficiency. The oil droplet surface is touched by SDBS surfactant micelles at 11 ns, and they diffuse to stick to the outside of the droplet. The SDBS molecules travel around the surface of crude oil in a clockwise direction when subjected to a water flow. More SDBS molecules then travel in the direction of the crude oil/rock interface, altering the droplet's shape. The crude oil gradually separates from the rock surface as a result of more water molecules entering the crude oil−rock interface during this process. After the simulation has run long enough, a water channel will eventually form where the water fills the rock's surface, causing the oil droplets to separate from the wall. The INT surface exhibits a small contact area between the oil droplets and the orifice surface, causing the droplets to move quickly on the surface as a result of water flow. As a result, it is discovered that when the oil droplets are not in contact with the surfactant, they deform.

Adsorption of surfactant and self-aggregation take place during the process of repelling oil with surfactant and water. The surfactant approaches the oil droplets in the direction of the water flow as the pusher plate moves to the right and adsorbs onto the droplets. The water molecules occupied the surface sites and loosened the oil molecules as a result of the surfactant molecules migrating to the backbone of the oil aggregate due to the action of the water flow. The configurations of the special moment points of the simulated trajectories are chosen for comparison based on the trajectory analysis of various oil-repellent systems (Figure 8). There are tiny DTAB aggregates that are more susceptible to the water flow effect and arrive at the oil/water interface faster. However, because SDBS forms two larger aggregates that increase flow resistance, it flows more slowly in the slit and takes longer to reach the oil−water interface. Second, some of the DTAB is adsorbed on a solid surface, which lowers the utilization rate of the DTAB surfactant. The O atom in SiO_2 surface OH is negatively charged, and the headgroup portion of the cationic surfactant is positively charged (Figure 9).

The study's main goal was to determine how oil moves in tandem with water flow by measuring the center of mass displacements of oil droplets in various orifices. The transport rate of oil droplets across various orifices varied significantly according to the results (see Figure 8). When a surfactant is added to the system, it forms an adsorption layer by covering the oil's surface. When used for the first time, technical term abbreviations like "adsorption layer" are defined. The oil droplets start to distort and slide up against the orifice wall as a result of the water flow. The combination of surfactant and water flow causes the oil droplets to advance on the wall at different simulation times. The migration speed of oil droplets is improved more when SDBS surfactant is added. Two surfactants were applied to the three surfaces during the simulation, and each surface showed a different speed. The INF surface showed the fastest oil droplet speed, which was followed by the CVFF surface and the COM surface. The oil droplet moved and displaced more effectively when there were more SDBS molecules affixed to its surface. An oil band forms close to the wall's surface as a result of the oil molecules diffusing across the surface more quickly. This oil band's larger surface area causes it to generate more resistance. As a result, it moves more slowly. Conversely, the oil droplets located in the COM and INF channels exhibit less deformation and have a reduced surface area in contact with the wall. As a result, the oil droplets travel faster and encounter less resistance from the wall surface.

3.3. Analysis of Oil Droplet Transport Behavior in Nanopore Channels. When surfactant is added to an oil system, it coats the oil's surface and forms an adsorption layer. When water flows through the system, the oil droplets start to deform and slide along the pore wall. This is caused by the surfactant altering the interfacial tension between the water and solid surfaces, which alters the wettability of the rock surface.[37] The adhesion force and its cohesion are the oil displacement resistances, and the shear force, rock adhesion force, and cohesion are the forces that the oil droplets encounter during displacement. Because surfactants permeate the wall and diffuse along it, they decrease the area of contact between the crude oil and the pore wall. Additionally, they alter the wall's structure to make it more hydrophilic, which lowers the adhesion force.[38] Crude oil readily separates from the wall as adhesion diminishes. The leading edge of the oil film only experiences cohesion and self-generated shear stress when the contact angle is less than 90 deg. The surfactant weakens the cohesiveness of the oil film. Because of the dispersing and depolymerizing effects of the surfactant system's shear force, the first surfactant to break off can disperse. The initial grouping of crude oil molecules disperses in the pore wall as a result of this process.

The CVFF system was used as an example to thoroughly investigate the transport mechanism of surfactant-encased oil droplets on the pore surface. Figure 10 displays the calculated

https://doi.org/10.1021/acsomega.3c09116
ACS Omega 2024, 9, 4085−4095

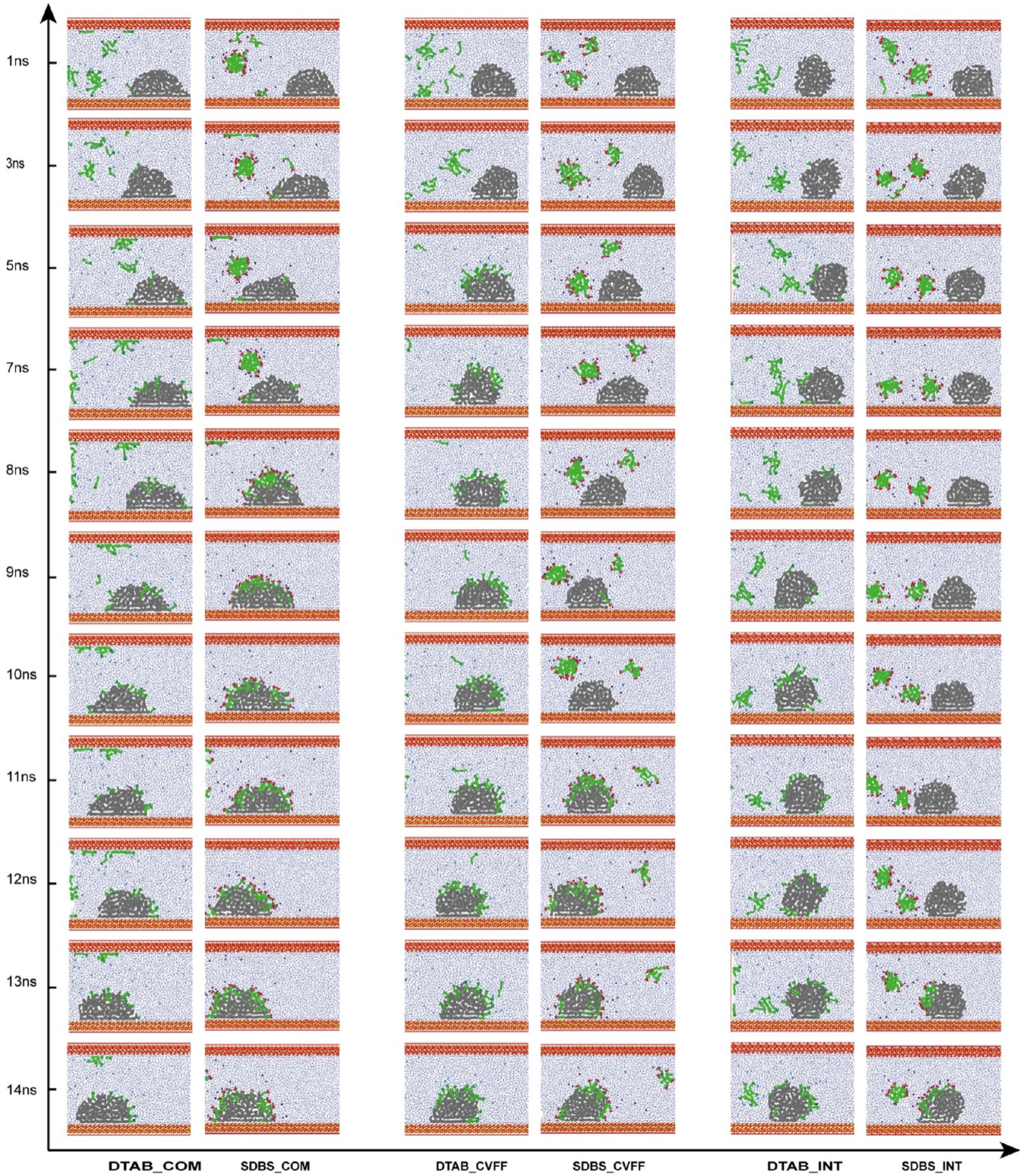

Figure 8. Adsorbed oil displacement during surfactant injection in a hydroxylated quartz nanochannel.

distribution of the water flow rate along the direction of the pore diameter. Despite the push plate's force, the water flow continues in the same direction. Nonetheless, flow resistance at the wall and strong interaction with the surfactant layer influence the directional diffusion of water in the orifice near the oil droplets, leading to a notable difference between the oil droplets and the upper and lower walls. The oil droplet and the orifice's lower wall surface constitute the main area of the water flow velocity distribution. A water channel forms when the space between the oil droplet and the surface is gradually filled with water as the droplet slowly separates from the solid surface. Through this channel, water molecules diffuse toward the surface. It is possible to approximate the hydrodynamic data in the nanopore channel by performing velocity

https://doi.org/10.1021/acsomega.3c09116
ACS Omega 2024, 9, 4085−4095

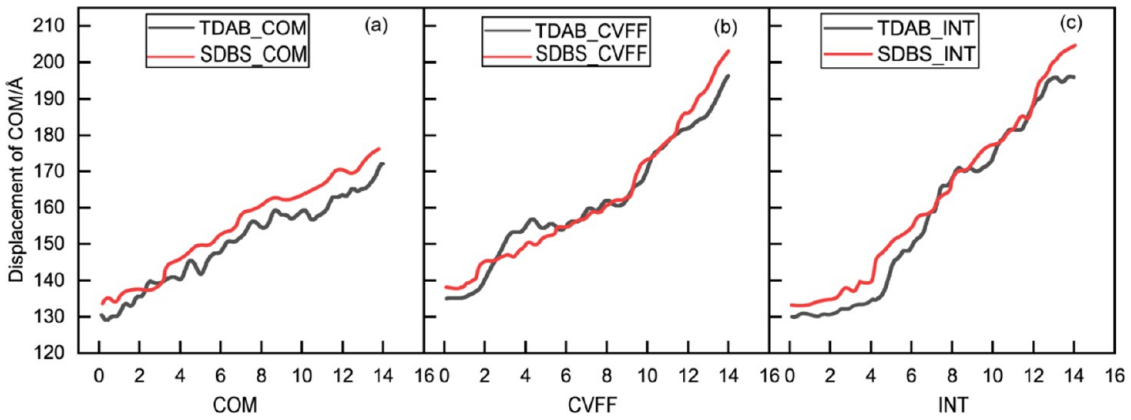

Figure 9. Center-of-mass (COM) displacement of the oil aggregate in the *X* direction under three surfaces: (a) COM surface, (b) CVFF surface, and (c) INT surface.

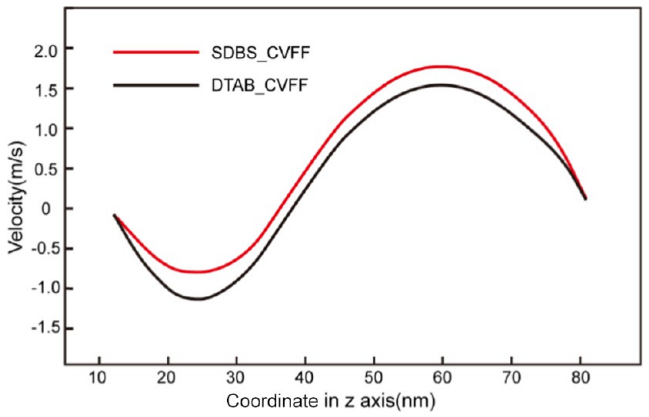

Figure 10. Velocity distribution of water across the aperture.

distribution calculations, as shown in Figure 11. The water flow is always flowing in the right direction during the simulation. Figure 10 illustrates the localized resistance near the oil droplets and the presence of a negative incoming velocity value near the lower wall surface, which causes a vortex to form in the opposite direction of the water flow. Here, the space is replaced with water as the oil droplet progressively separates from the solid surface and forms a water channel between it and the surface. The channel allows water molecules to diffuse toward the surface, and as it expands, it helps the oil droplet separate from the surface. Water eventually accumulates on the oil droplet's surface from both sides, covering it completely. The oil droplet separates from the wall as a single unit as a result of this process.

3.4. Interaction of Substrate Polarity with Water Molecules. This section looks at how the substrate polarity affects oil repulsion. van der Waals forces involve noncovalent, short-range interactions between molecules, whereas Coulomb interactions involve long-range interactions between charges. We assess the Coulomb interaction between an atomically charged silica surface and a water molecule, as shown in Figure 12. The Coulombic interaction between the water molecule and the silica surface is significantly larger for more polar substrates (interface in Table 1) than it is for less polar substrates (COMPASS, CVFF in Table 1), and it is also significantly larger than the Coulombic interaction between the water molecule and the silica surface. Simulations reveal that the formation of water molecule channels is significantly influenced by electrostatic interactions between water molecules and polar substrates. Water molecule channels are more likely to form for the more polar silica substrate. This further clarifies why the oil phase in the stronger polar substrate (COMPASS, CVFF in Table 1) is a spherical oil droplet and the oil phase in the weaker polar substrate (compass) is a flat oil layer. The main bond in the structure of silica is called the silicon−oxygen bond (Si−O), and it is made up of two atoms: silicon and oxygen. Because the silicon atom is more electropositive and the oxygen atom is more electronegative, this bond is typically polar. The silicon−oxygen bond therefore displays some polarity. Because of their polarity, silicon−oxygen bonds tend to interact with water molecules, making them somewhat hydrophilic. Because water molecules are

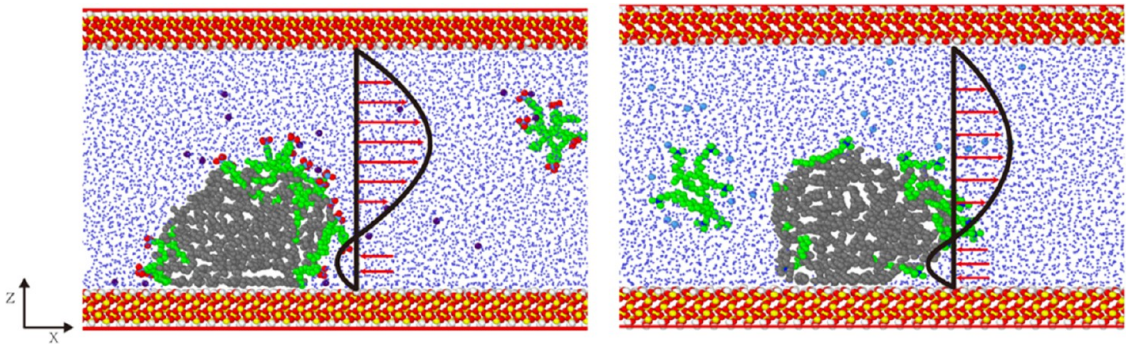

Figure 11. Flow velocity distribution of water in 14 ns.

https://doi.org/10.1021/acsomega.3c09116
ACS Omega 2024, 9, 4085−4095

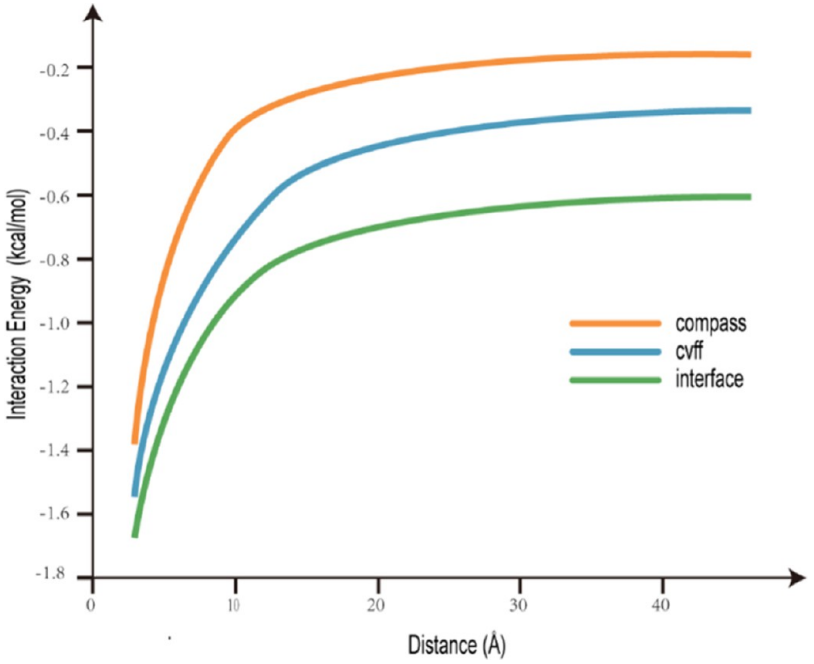

Figure 12. Coulomb interaction between a silica surface and a water molecule.

polar, meaning they are made up of two hydrogen atoms and one oxygen atom, they have a positively charged oxygen atom and a negatively charged hydrogen atom. When water molecules interact with the silica−oxygen bonds on the surface of silica, hydrogen bonds may form. A hydrogen atom interacting with a weaker bond between a more electronegative atom (typically oxygen, nitrogen, or fluorine) is known as hydrogen bonding. This interaction may cause water molecules to adsorb to the silicon surface in the case of silicon−oxygen bonds and water molecules.

4. CONCLUSIONS

This study utilizes an all-atom force field for molecular dynamics simulations to investigate the mechanism of crude oil propulsion in hydrophilic nanopores. In conjunction with the practical situation, we added two surfactants to the solution and measured the static contact angle to elaborate the adsorption state of oil droplets on different surfaces by observing the change in oil droplet shape. Finally, it was concluded that the strongly polar surface (INT) has a smaller contact angle and the oil droplets move more easily in the pores, thus having better repulsion efficiency. After that, we studied the whole oil expulsion process in detail, the water flow rate near the wall surface, the factors of water channel formation, etc. Finally, we showed that surfactants play a role in EOR: increase the perturbation of oil molecules on the wall surface, which in turn reduces the contact area of oil molecules with the wall to ensure that the oil molecules can move quickly on the wall surface; surfactants can better open the water channel, and after that, more water molecules enter between the oil and the wall. We also examined the interaction between each rock surface and the water molecules, of which electrostatic interaction is the main part, and the stronger the polarity, the stronger the interaction with the water molecules.

This study aims to analyze the influence of surfactants on the solid−liquid interface properties during oil displacement and the resulting variations in displacement outcomes. The research aims to analyze the oil displacement process within nanoscale pores of reservoir media from a microscopic perspective, providing a theoretical basis for selecting surfactants in different wetting environments.

Molecular simulations can provide insight into EOR processes at the molecular level. They can guide scientists and engineers to effectively improve oil recovery.

AUTHOR INFORMATION

Corresponding Author

Kaili liao − *School of Petroleum and Natural Gas Engineering, School of Energy, Changzhou University, Changzhou 21306, China;* orcid.org/0000-0003-2720-9579; Email: lkl123@163.com

Authors

Lipei Fu − *School of Petroleum and Natural Gas Engineering, School of Energy, Changzhou University, Changzhou 21306, China;* orcid.org/0000-0001-5294-5223

Yuan Cheng − *School of Petroleum and Natural Gas Engineering, School of Energy, Changzhou University, Changzhou 21306, China*

Zhanqi Fang − *School of Petroleum and Natural Gas Engineering, School of Energy, Changzhou University, Changzhou 21306, China*

Minglu Shao − *School of Petroleum and Natural Gas Engineering, School of Energy, Changzhou University, Changzhou 21306, China;* orcid.org/0000-0003-1249-0601

Jiyun Zhu − *School of Petroleum and Natural Gas Engineering, School of Energy, Changzhou University, Changzhou 21306, China*

Ziqiang Xu − *Oil And Gas Technology Research Institute Changqing Oilfield Company, PetroChina, Xi'an 710018, China*

https://doi.org/10.1021/acsomega.3c09116
ACS Omega 2024, 9, 4085−4095

Yanyu Xu − *School of Petroleum and Natural Gas Engineering, School of Energy, Changzhou University, Changzhou 21306, China*

Complete contact information is available at: https://pubs.acs.org/10.1021/acsomega.3c09116

Notes

The authors declare no competing financial interest.

■ ACKNOWLEDGMENTS

The authors are grateful for funding from the China Postdoctoral Science Foundation (no. 2022M721396), the Major Project of Universities Affiliated to Jiangsu Province Basic Science (Natural Science) Research (23KJA440001), the Basic Science (Natural Science) Research Projects of Colleges and Universities in Jiangsu Province (no. 22KJB440001), the Natural Science Foundation of Jiangsu Province (no. BK20220622), the Industry-University-Research Collaboration Program supported by Science and Technology Department of Jiangsu Province (BY2022963), the Sci & Tech Program of Changzhou (no. CE20225065), the Postgraduate Research & Practice Innovation Program of Jiangsu Province (no. SJCX23_1564), and the Jiangsu Students' Innovation and Entrepreneurship Training Program (nos. 202310292108Y, 202310292166A, 202310292165A, and 202310292213B).

■ REFERENCES

(1) McAuliffe, C. D. Oil and Gas Migration—Chemical and Physical Constraints. *AAPG Bull.* **1979**, *63* (5), 761−781.

(2) Harry Dembicki, J.; Anderson, M. J. Secondary Migration of Oil: Experiments Supporting Efficient Movement of Separate, Buoyant Oil Phase Along Limited Conduits. *AAPG Bull.* **1989**, *73* (8), 1018−1021.

(3) Dandekar, A. Y. *Petroleum Reservoir Rock and Fluid Properties*, CRC Press: Boca Raton, 2013.

(4) Peters, K. E.; Fowler, M. G. Applications of Petroleum Geochemistry to Exploration and Reservoir Management. *Org. Geochem.* **2002**, *33* (1), 5−36.

(5) Liu, K.; Ostadhassan, M.; Zhou, J.; Gentzis, T.; Rezaee, R. Nanoscale Pore Structure Characterization of the Bakken Shale in the USA. *Fuel* **2017**, *209*, 567−578.

(6) Esfe, M. H.; Hosseinizadeh, E.; Esfandeh, S. Flooding Numerical Simulation of Heterogeneous Oil Reservoir Using Different Nanoscale Colloidal Solutions. *J. Mol. Liq.* **2020**, *302*, No. 111972.

(7) Luo, S.; Lutkenhaus, J. L.; Nasrabadi, H. Effect of Nanoscale Pore-Size Distribution on Fluid Phase Behavior of Gas-Improved Oil Recovery in Shale Reservoirs. *SPE J.* **2020**, *25* (03), 1406−1415.

(8) Kumar, M.; Middleton, J. P.; Sheppard, A.; Senden, T.; Knackstedt, M. A. Quantifying Trapped Residual Oil in Reservoir Core Material at the Pore Scale: Exploring the Role of Displacement Rate, Saturation History and Wettability. In *International Petroleum Technology Conference*, cp-151-00321, 2009.

(9) Kunieda, M.; Nakaoka, K.; Liang, Y.; Miranda, C. R.; Ueda, A.; Takahashi, S.; Okabe, H.; Matsuoka, T. Self-Accumulation of Aromatics at the Oil−Water Interface through Weak Hydrogen Bonding. *J. Am. Chem. Soc.* **2010**, *132* (51), 18281−18286.

(10) Ghatee, M. H.; Fotouhabadi, Z.; Zolghadr, A. R.; Borousan, F.; Ghanavati, F. Structural and Phase Behavior Studies of Pyridine and Alkyl Pyridine at the Interface of Oil/Water by Molecular Dynamics Simulation. *Ind. Eng. Chem. Res.* **2013**, *52* (37), 13384−13392.

(11) Kovalchuk, N. M.; Simmons, M. J. H. Surfactant-Mediated Wetting and Spreading: Recent Advances and Applications. *Curr. Opin. Colloid Interface Sci.* **2021**, *51*, No. 101375.

(12) Schweighofer, K. J.; Essmann, U.; Berkowitz, M. Simulation of Sodium Dodecyl Sulfate at the Water−Vapor and Water−Carbon Tetrachloride Interfaces at Low Surface Coverage. *J. Phys. Chem. B* **1997**, *101* (19), 3793−3799.

(13) Li, H.; Dai, C.; Wu, X. *Developing New Recyclable and Ph-Sensitive Amphiphile for Heavy Oil Emulsion and Demulsification: A Molecular Dynamics Study*; Springer, 2019; pp 1063−1073.

(14) Ahmadi, M.; Aliabadian, E.; Liu, B.; Lei, X.; Khalilpoorkordi, P.; Hou, Q.; Wang, Y.; Chen, Z. Comprehensive Review of the Interfacial Behavior of Water/Oil/Surfactant Systems Using Dissipative Particle Dynamics Simulation. *Adv. Colloid Interface Sci.* **2022**, *309*, No. 102774.

(15) Shi, P.; Zhang, H.; Lin, L.; Song, C.; Chen, Q.; Li, Z. Molecular Dynamics Simulation of Four Typical Surfactants at Oil/Water Interface. *J. Dispersion Sci. Technol.* **2018**, *39* (9), 1258−1265.

(16) Mohan, K.; Gupta, R.; Mohanty, K. K. Wettability Altering Secondary Oil Recovery in Carbonate Rocks. *Energy Fuels* **2011**, *25* (9), 3966−3973.

(17) Salehi, M.; Johnson, S. J.; Liang, J.-T. Mechanistic Study of Wettability Alteration Using Surfactants with Applications in Naturally Fractured Reservoirs. *Langmuir* **2008**, *24* (24), 14099−14107.

(18) Aranda-Bravo, C. G.; Méndez-Bermúdez, J. G.; Dominguez, H. Desorption of Decane Molecules from a Graphite Surface Produced by Sodium Alpha Olefin Sulphate/Betaine Surfactant Mixtures: A Computer Simulation Study. *J. Mol. Liq.* **2014**, *200*, 465−473.

(19) Kolev, V. L.; Kochijashky, I. I.; Danov, K. D.; Kralchevsky, P. A.; Broze, G.; Mehreteab, A. Spontaneous Detachment of Oil Drops from Solid Substrates: Governing Factors. *J. Colloid Interface Sci.* **2003**, *257* (2), 357−363.

(20) Zhang, H.; Nikolov, A.; Wasan, D. Dewetting Film Dynamics inside a Capillary Using a Micellar Nanofluid. *Langmuir* **2014**, *30* (31), 9430−9435.

(21) Li, X.; Xue, Q.; Wu, T.; Jin, Y.; Ling, C.; Lu, S. Oil Detachment from Silica Surface Modified by Carboxy Groups in Aqueous Cetyltriethylammonium Bromide Solution. *Appl. Surf. Sci.* **2015**, *353*, 1103−1111.

(22) Druetta, P.; Picchioni, F. Surfactant Flooding: The Influence of the Physical Properties on the Recovery Efficiency. *Petroleum* **2020**, *6* (2), 149−162.

(23) Tavakkoli, O.; Kamyab, H.; Shariati, M.; Mohamed, A. M.; Junin, R. Effect of Nanoparticles on the Performance of Polymer/Surfactant Flooding for Enhanced Oil Recovery: A Review. *Fuel* **2022**, *312*, No. 122867.

(24) Liu, J.; Zhong, L.; Hao, T.; Liu, Y.; Zhang, S. Pore-Scale Dynamic Behavior and Displacement Mechanisms of Surfactant Flooding for Heavy Oil Recovery. *J. Mol. Liq.* **2022**, *349*, No. 118207.

(25) Nafisifar, A.; Manshad, A. K.; Shadizadeh, S. R. Primary Evaluation of a New Green Synthesized Anionic Surfactant, Micellar Behavior Analysis, and Flooding in Sandstone Reservoirs: Application in Chemical Enhanced Oil Recovery. *SPE J.* **2022**, *27* (01), 771−789.

(26) Jang, S. S.; Lin, S.-T.; Maiti, P. K.; Blanco, M.; Goddard, W. A.; Shuler, P.; Tang, Y. Molecular Dynamics Study of a Surfactant-Mediated Decane−Water Interface: Effect of Molecular Architecture of Alkyl Benzene Sulfonate. *J. Phys. Chem. B* **2004**, *108* (32), 12130−12140.

(27) Tang, X.; Xiao, S.; Lei, Q.; Yuan, L.; Peng, B.; He, L.; Luo, J.; Pei, Y. Molecular Dynamics Simulation of Surfactant Flooding Driven Oil-Detachment in Nano-Silica Channels. *J. Phys. Chem. B* **2019**, *123* (1), 277−288.

(28) Tang, J.; Qu, Z.; Luo, J.; He, L.; Wang, P.; Zhang, P.; Tang, X.; et al. Molecular Dynamics Simulations of the Oil-Detachment from the Hydroxylated Silica Surface: Effects of Surfactants, Electrostatic Interactions, and Water Flows on the Water Molecular Channel Formation. *J. Phys. Chem. B* **2018**, *122* (6), 1905−1918, DOI: 10.1021/acs.jpcb.7b09716.

(29) Takamura, K.; Chow, R. S. The Electric Properties of the Bitumen/Water Interface Part Ii. Application of the Ionizable Surface-Group Model. *Colloids Surf.* **1985**, *15*, 35−48.

(30) Yan, Y.-L.; Cui, M.-Y.; Jiang, W.-D.; He, A.-L.; Liang, C. Drag Reduction in Reservoir Rock Surface: Hydrophobic Modification by SiO_2 Nanofluids. *Appl. Surf. Sci.* **2017**, *396*, 1556−1561.
(31) Sun, H. Compass: An Ab Initio Force-Field Optimized for Condensed-Phase Applicationssoverview with Details on Alkane and Benzene Compounds. *J. Phys. Chem. B* **1998**, *1998*, 7338−7364.
(32) Dauber-Osguthorpe, P.; Roberts, V. A.; Osguthorpe, D. J.; Wolff, J.; Genest, M.; Hagler, A. T. Structure and Energetics of Ligand Binding to Proteins: *Escherichia Coli* Dihydrofolate Reductase-Trimethoprim, a Drug-Receptor System. *Proteins: Struct., Funct., Bioinf.* **1988**, *4* (1), 31−47, DOI: 10.1002/prot.340040106.
(33) Heinz, H.; Lin, T.-J.; Kishore Mishra, R.; Emami, F. S. Thermodynamically Consistent Force Fields for the Assembly of Inorganic, Organic, and Biological Nanostructures: The Interface Force Field. *Langmuir* **2013**, *29* (6), 1754−1765.
(34) Martínez, L.; Andrade, R.; Birgin, E. G.; Martinez, J. M. Packmol: A Package for Building Initial Configurations for Molecular Dynamics Simulations. *J. Comput. Chem.* **2009**, *30* (13), 2157−2164, DOI: 10.1002/jcc.21224.
(35) Berendsen, H. J. C.; Grigera, J. R.; Straatsma, T. P. The Missing Term in Effective Pair Potentials. *J. Phys. Chem. A* **1987**, *91* (24), 6269−6271.
(36) Plimpton, S. Fast Parallel Algorithms for Short-Range Molecular Dynamics. *J. Comput. Phys.* **1995**, *117* (1), 1−19.
(37) Liu, Z.; Jiao, L.; Yang, H.; Zhu, M.; Zhang, M.; Dong, B. Study on the Microstructural Characteristics of Coal and the Mechanism of Wettability of Surfactant Solutions at Different Ph Levels. *Fuel* **2023**, *353*, No. 129268.
(38) Brumaru, C.; Geng, M. L. Interaction of Surfactants with Hydrophobic Surfaces in Nanopores. *Langmuir* **2010**, *26* (24), 19091−19099.

https://doi.org/10.1021/acsomega.3c09116
ACS Omega 2024, 9, 4085−4095